RESEARCH ARTICLE
Optimisation of support stiffness at railway crossings

I. Grossoni[1a], Y. Bezin[2 a], S. Neves[3 a]

[a] *Institute of Railway Research, University of Huddersfield, Huddersfield, UK*

Abstract

Turnouts are a key element of the railway system. They are also the part of the system with the highest number of degradation modes and associated failures. There are a number of reasons for this, including high dynamic loads resulting from non-uniform rail geometry and track support stiffness. The main aim of this study is to propose a methodology to optimise the pad stiffness along a crossing panel in order to achieve a decrease in the indicators of the most common failure modes. A three-dimensional vehicle/track interaction model has been established, considering a detailed description of the crossing panel support structure. A genetic algorithm has been applied to two main types of constructions, namely direct and indirect fixing, to find the optimum combinations of resilient pad characteristics for various cases of travelling direction, travelling speed and support conditions.

Keywords

Crossing panel; support stiffness; fixing systems; design optimisation; vehicle/track interaction model

1. Introduction

Switches and Crossings (S&Cs), also called turnouts, refer to the components of the railway that provide flexibility to the system in terms of possible route change as they are the only locations at which routes cross, converge or diverge and, thus, trains can change path. Therefore, the performance of the entire line is deeply influenced by the number and types of its turnouts [1]. Turnouts are one of the parts of the railway system with the highest number of failures [2]. The reasons are numerous, such as non-ideal wheel transition over the load transfer area due to poor rail geometry, high curvature in contact zone and too short transitions. Furthermore, there is a significant longitudinal variation of the vertical support stiffness along the switch and the crossing panel, which contributes to further vibrations and acceleration in the track degradation processes. This change of characteristics may be partially controlled by choosing appropriate support stiffness elements in order to obtain an overall rigidity as smooth as possible through the S&C.

Although this problem has been partially addressed, it is far from being entirely solved. For example, in Nicklisch [3] a methodology to optimise support stiffness at the switch panel has been proposed varying the rail-pad properties or applying under sleeper pads (USPs). The highest reductions are found using stiffer pads in the plane line and softer pads close to the switch heel. This arrangement leads to a significant reduction in the wear index T-gamma. However, other quantities of interest are not looked at in detail, particularly the reduction of forces in the track elements. In the crossing panel the support stiffness is only briefly analysed, acknowledging high potential for the reduction of material degradation of the crossing nose. Within the EU Project INNOTRACK ([4, 5]), measured maximum vertical forces with two different pads

[1] Corresponding author: Ilaria Grossoni, Institute of Railway Research, University of Huddersfield, Queensgate, Huddersfield HD1 3DH, West Yorkshire, United Kingdom. Email: i.grossoni@hud.ac.uk. Telephone: +44 (0)1484 471179

[2] Yann Bezin, Email: y.bezin@hud.ac.uk Telephone: +44 (0)1484 473732

[3] Sergio Neves, Email: s.neves@hud.ac.uk Telephone: +44 (0)1484 478751

and varying speed have been presented. When the through route is considered, the case with soft pads shows lower contact forces than the case with stiff pads for all the speeds investigated. On the contrary, when the diverging route is considered, this is not always true. In Markine [6], three design parameters, that are the stiffness and the damping of rail-pads and the sleeper weight, have been considered to optimize the crossing performance in terms of vertical dynamic forces, which are responsible for rolling contact fatigue (RCF) related damage of the crossing nose and wing rails. USPs are also considered in the paper to help reduce the dynamic impact loads. Results show that the best performance of the turnout is achieved using very soft pads in combination with USPs increasing the total resilience of the track form. These findings are in agreement with Bruni [7], where a sensitivity analysis has been performed considering nine different cases and including rail profile correction, USPs and ballast mats. In particular, the corrected profile refers to an improved rail geometry providing 75 % reduction of vertical wheel displacement during the passage over the crossing nose. Site experiments performed within the EU Project SUSTRAIL [8] show that USPs provide a positive influence on ballast conditions, reducing abrasion, eliminating the formation stiffness influence and improving the uniformity of system stiffness. An automated routine to optimise the dynamic performance of railway crossings varying the track resilience has been established in Wan [9]. One counter argument however, is highlighted by measurements of vertical ground vibrations at turnouts carried out within the EU Project RIVAS ([10]) showing that USPs can also increase the vibration levels. It is however not possible to draw definitive conclusions due to poor reproducibility of experiments. Overall it would seem that USP are good to protect the ballast and homogenise the stiffness of the track, but too low modulus should not be used to avoid risk of increased vibration.

Both experiments and numerical models show that a significant reduction in wheel/rail contact forces can be gained using increased system resilience. Also, adding USPs can further enhance the performances at the crossing panel. Therefore, it is recognised that the overall track system stiffness plays a fundamental role in the dynamic response of the vehicle/track system. Nevertheless, changes in individual component's resilience and their combinations have not been systematically studied and understood to ensure that their effect on the track system response is acceptable (frequency and phase response). Also, the vehicle/track interaction response has not been entirely examined so far in literature in relation with track degradation modes. There are currently no strict specifications or guidelines on rail-pad stiffness to be installed in a crossing panel as function of its intended usage, i.e. track category and support quality and traffic type (speed and tonnage). The main aim of this work is to understand the influence of the fixing system on the overall crossing performance, investigating the major degradation mechanisms occurring at the crossing panel and proposing a detailed recommendation for the pad properties.

In Section 2, the fixing systems at railway crossings are briefly discussed. A detailed analysis of track systems at crossing panel is then carried out in Section 3, comparing different fixing systems in terms of frequency response and static stiffness. The influence of USPs is also analysed. In Section 4 a genetic algorithm (GA) is applied to find an optimum design solution in terms of support stiffness for specific cases strictly related to standard UK S&C designs. The objective function is based on damage levels that account for rolling contact fatigue (RCF), wear, settlement and fatigue in the components. The trend of each indicator is discussed in detail. A three-dimensional vehicle/track interaction model is established and used to calculate the dynamic behaviour at the crossing panel. A first comparison of optimum solutions is presented in Section 5. Finally, in Section 6 a parametric study is carried out in order to establish the influence of track parameters (i.e. support stiffness) and vehicle parameters (i.e. speed and travelling direction) on the optimum solution.

2. Fixing systems at railway crossings

Pads are required to help maintain the track geometry, to provide impact protection of components, in particular at the interface between rail and sleeper, to prevent component wear, to provide electrical insulation and resistance to rail creep and to contribute to minimise noise and vibration emissions [11].

In the railway system, there are two main ways to link the rail to the sleeper: direct fastening (i.e. the rail and the sleeper are directly connected through rail-pads) and indirect fastening (between the rail and

the sleeper there is the baseplate system, which includes a rail-pad and a baseplate-pad). In the UK network, the direct fastening is usually used with crossings with 56E1 profile as reference rail and the indirect fastening with crossings with 60E1 or 60E2 profile as reference rail. Examples are shown in Figure 1.

Figure 1. Example of (a) direct fixing and (b) indirect fixing.

The dynamic performance of the system is strictly depending on the stiffness properties of the fixing. Therefore, it is necessary to use a standardised method to perform tests and characterise the properties. The pad static stiffness assessment and the pad dynamic stiffness assessment are described in the Euro Norm EN13146 [12].

In Euro Norm EN14363 [13], it is stated that the pad low frequency dynamic stiffness and the assembly high frequency dynamic stiffness can be required by the purchaser. Also, the loads are given according to the relevant European standard ([14-17]). Focusing on the case of concrete sleepers as relevant for this study, the loads for measurement of stiffness are given depending on the fastening category, which is defined depending on the maximum axle load and the minimum curve radius. The pad behaviour should be tested also under the effect of repeated loading. The change in performance before and after repeated loading must not exceed the maximum changes given for longitudinal rail restraint (change ≤20 %), vertical stiffness (change ≤25 %) and clamping force (change ≤20 %). Note that the requirement for change in vertical static stiffness is not applicable to fastening systems with a static stiffness greater than 300 KN/mm.

Typical values of static and dynamic rail-pad vertical stiffness have been collected from the manufactures technical information sheets and classified depending on the pad type (see Table 1). It is common to use soft pads (micromax pads) in case of direct fixing and use hard pads (Ethylene Vinyl Acetate (EVA) pads) in series with very soft baseplate-pads (such as rubber bonded cork (RBC) pads) in case of indirect fixing [18]. In particular, EVA pads are classified as type C (i.e. pad for specific circumstances where softer pads may give inacceptable dynamic gauge widening or acoustic performance) and RBC as type A (i.e. pad with high impact attenuation properties) [11].

Table 1. Static and dynamic stiffness of rail-pads and baseplate-pads (equivalent to 140 X 140 mm pad).

Description	Thickness [mm]	Static stiffness [kN/mm]	Dynamic stiffness [kN/mm]	Dynamic/static ratio	Pad type
Rail-pad	5.5-10.5	50-120	80-200	1.2-2.4	Soft pad
	5-10	150-520	200-1300	1.5-3	Medium pad
	5	550	-	-	Hard pad
Baseplate-pad	5-10	15-30	20-40	1.3	-
	3-5	50-80	90-140	1.8	-

3. Analysis of track systems in terms of static stiffness and frequency response

For the case of direct fixing, the track model is described in detail in Grossoni [19].

For the case of indirect fixing, a representation is shown in Figure 2. In this study, only the through route (highlighted in green in Figure 2c) is analysed.

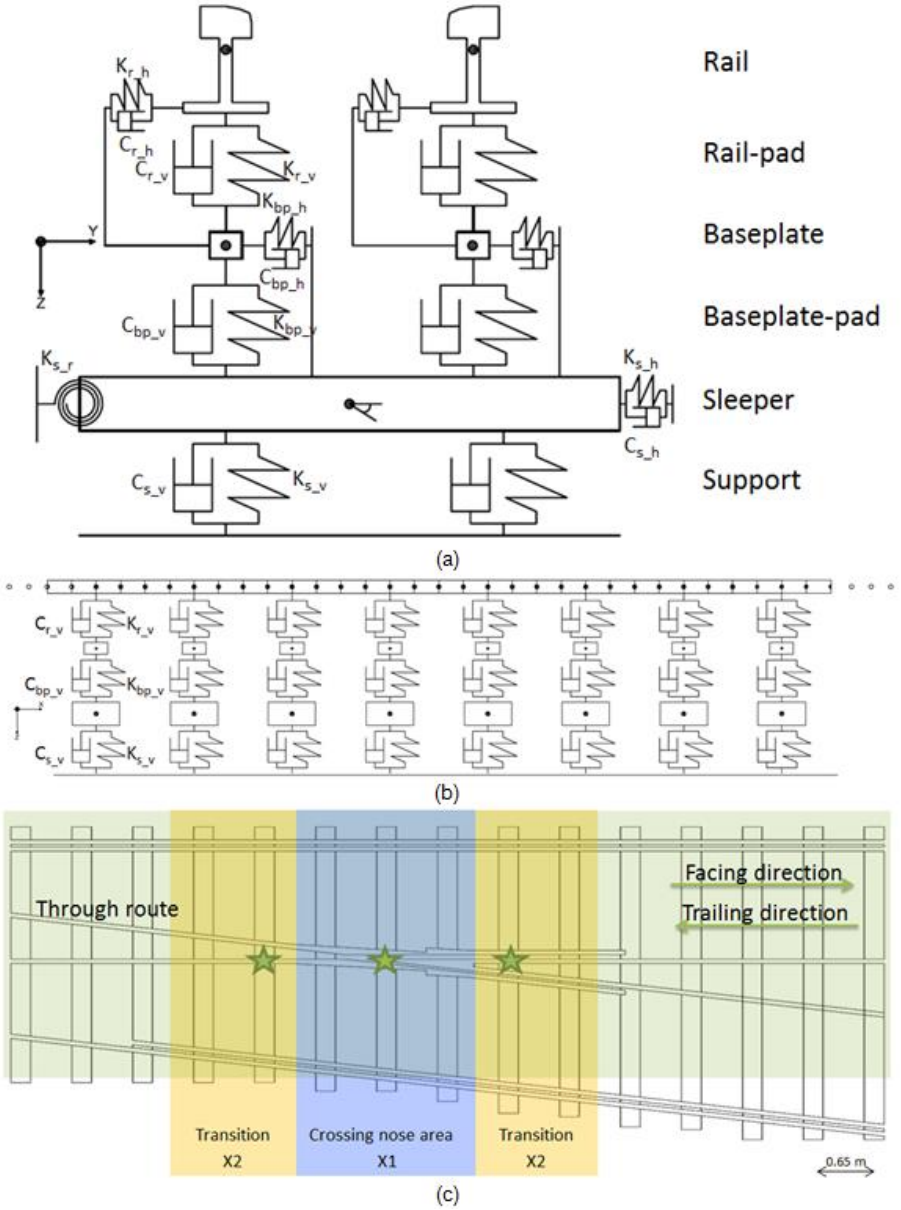

Figure 2. Track model in (a) y-z plane, (b) x-z plane and (c) x-y plane (indirect fixing).

The track is modelled as a three-layer discretely supported ballasted track, which includes the rail-pad, the baseplate-pad and the sleeper support resilient layers. Each rail node has four degrees of freedom

(DOFs): vertical and lateral displacement and rotations around the y and z axes (rail twist is neglected here). In order to obtain accurate results and capture appropriately the abrupt change in the crossing geometrical properties, four Timoshenko beam elements are considered within each sleeper-spacing. The baseplates and sleepers are modelled as rigid bodies with 2 DOFs (i.e. vertical and lateral displacement) and 3 DOFs (i.e. vertical and lateral displacement and roll rotation), respectively. In addition to the vertical and lateral support, an equivalent roll spring is considered to replicate the roll resistance of the long bearers.

Note that the track properties, including the sleeper length, support stiffness, rail-pad/baseplate-pad stiffness and rail properties, are variable along the crossing panel, matching the site general arrangement and the crossing panel drawings. In particular, the support and the rail-pad/baseplate-pad stiffness are function of the sleeper surface area and the foot width, respectively. Moreover, the additional check rails and the diverging rails are modelled as additional localised masses and considering additional bending stiffness.

In the following Sections, two crossings which are widely installed in the UK network (namely CEN56 and NR60) are compared in terms of track response in the frequency domain (i.e. receptance) at various locations and static stiffness along the crossing panel. The main input parameters are listed in Table 2.

Table 2. Main input parameters for the two crossing types considered.

Parameter	CEN56	NR60
Rail type	56E1	60E1
Sleeper type	Concrete	Concrete
Crossing angle (1inN)	13	11
Sleeper spacing	0.71 m	0.65 m
Baseplate system	No	Yes
Rail/sleeper pad stiffness	81 kN/mm	-
Rail/baseplate-pad stiffness	-	550 kN/mm
Baseplate/sleeper pad stiffness	-	40 kN/mm
Support stiffness	60 kN/mm/m^2	60 kN/mm/m^2
Rail/sleeper pad damping	162 kNs/m	-
Rail/baseplate-pad damping	-	12 kNs/m
Baseplate/sleeper pad damping	-	15 kNs/m
Support stiffness damping	46.5 kNs/m	60 kNs/m

The values of the pads (i.e. rail and baseplate-pads) are given in accordance to the NR standard NR/L2/TRK/2049 [18] and the ballast support stiffness corresponds to typical track bed ([20]).

3.1. Track stiffness along the crossing panel

The global track stiffness K(s) at the position s along the track is calculated by performing a quasi-static analysis with a unit load applied above each sleeper. Figure 3 shows the comparison of CEN56 and NR60 designs in terms of stiffness along the crossing panel.

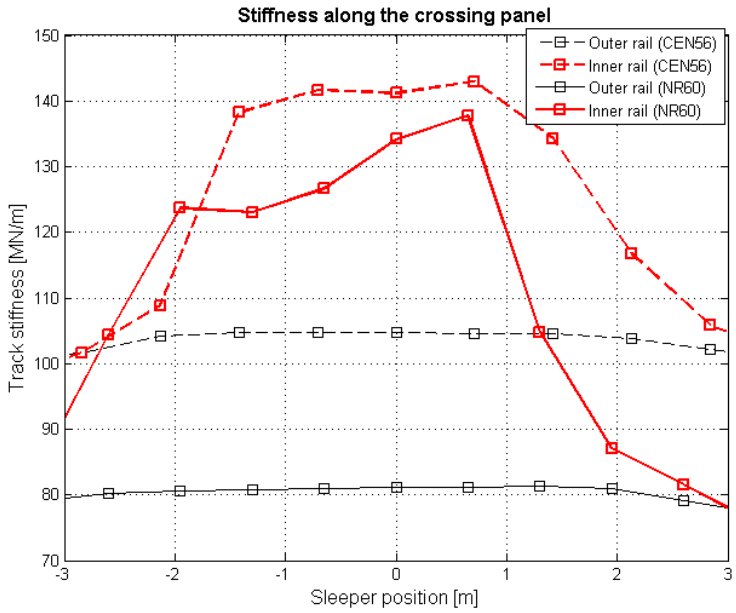

Figure 3. Comparison of CEN56 and NR60 crossings in terms of static stiffness along the crossing panel. The reference position is the crossing nose and the positive direction the facing direction of the through route.

First of all, in both cases it is possible to notice a remarkable increase of the track stiffness along the crossing panel. This can be explained with the significantly higher bending properties of the casting as well as the presence of long bearers and additional rails.

Comparing the distribution of static stiffness for the two designs in Figure 3, it is possible to see that there is an average decrease of ca. 5 % of stiffness for NR60 in comparison with CEN56 in case of inner rail and ca. 23 % in case of outer rail. This can be explained with the fact that the increased bending properties of the design are partially counterbalanced by the higher resilience given by the baseplate system.

In the NR standard RT/CE/S/052 [11], an estimation of the track stiffness is given based on the Beam On Elastic Foundation (BOEF) method. Considering the fact that the effective foundation modulus varies with axle load and considering a rail Young's modulus equal to 180 GPa, the resultant values of track stiffness are 152 KN/mm for 56E1 compatible crossings and 160 KN/mm for 60E1 compatible crossings. The relative difference is ca. 7.2 %.

3.2. Frequency response curves

In the frequency domain, assuming stationary harmonic vibration, the equations of the vertical motion can be written as:

$$(-\omega^2[M] + i\omega[C] + [K])\hat{z}(\omega) = \hat{F}(\omega) \tag{1}$$

Where ω is the frequency of excitation, $\hat{z}(\omega)$ the amplitude of the complex-valued displacement and $\hat{F}(\omega)$ the amplitude of the complex-valued input force.

Track receptance H(ω) at frequency ω is then calculated as:

$$H(\omega) = abs\left(\frac{\hat{z}(\omega)}{\hat{F}(\omega)}\right) = \frac{1}{(-\omega^2[M] + i\omega[C] + [K])} \tag{2}$$

The comparison of CEN56 and NR60 in terms of receptance at the crossing nose is shown in Figure 4.

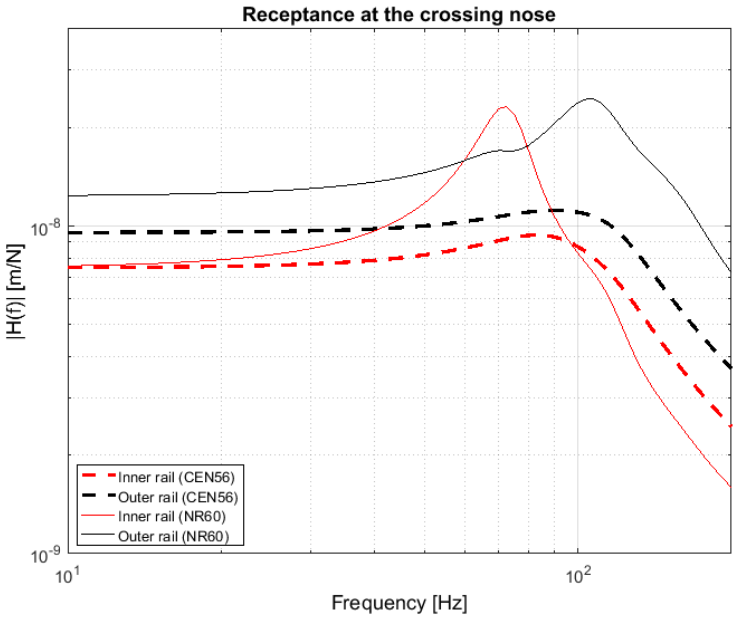

Figure 4. Comparison of CEN56 and NR60 crossings in terms of receptance at the crossing nose.

At low frequency (up to 30 Hz), the inner rail of both designs shows similar stiffness, as pointed out in Section 3.1. Towards higher frequencies, there is a 1st resonance peak which corresponds to the entire track (rails + sleeper) moving in phase against the ballast support stiffness. For the NR60 this appears at a slightly lower frequency (ca. 70Hz inner rail) due to increased mass and increased resilience in comparison with the CEN56 (ca. 100Hz inner rail). This difference is evident for the inner rail and rather negligible for the outer. Also noteworthy, the first resonant frequency magnitude response is higher for the NR60 than that of the CEN56 and less damping is present (sharper peak shape). This can be explained with the fact that the latter crossing is characterised by stiffer fixing system.

3.3. The influence of Under Sleeper Pads (USPs)

Three USP stiffness values (low stiffness: 100 kN/mm/m^2; medium stiffness: 150 kN/mm/m^2; high stiffness: 200 kN/mm/m^2) have been considered in this study.

Figure 5 shows the effect of USPs on the overall track stiffness of both CEN56 and NR60 crossing designs.

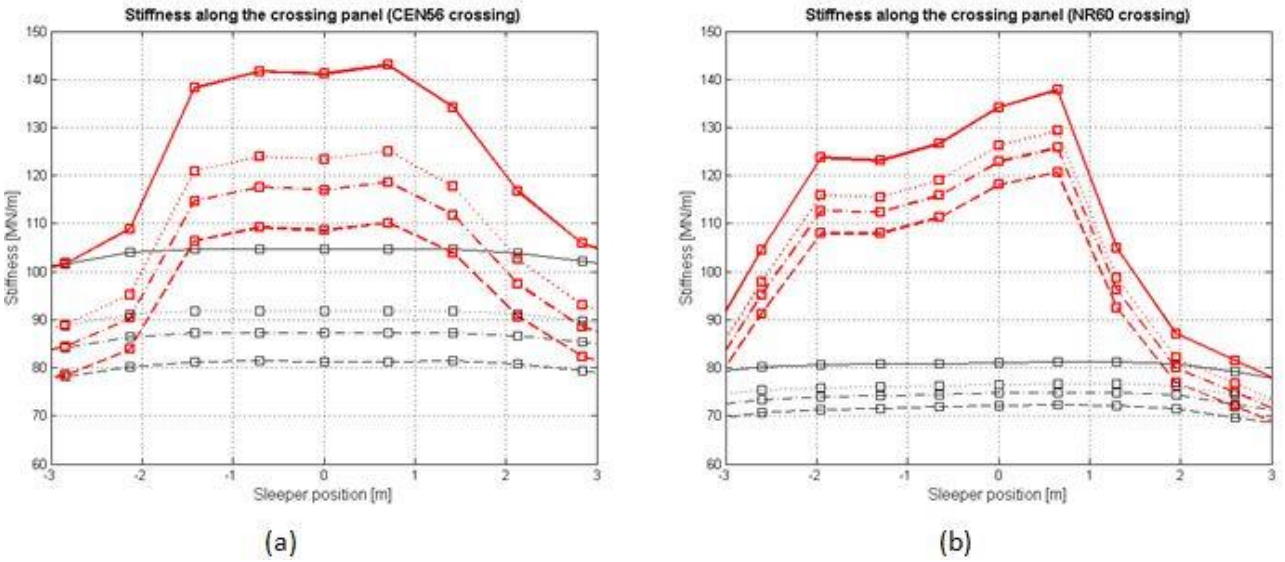

Figure 5. The effect of USPs on the overall track stiffness in case of (a) CEN56 crossing and (b) NR60 crossing (—: no USP, outer rail; — —: K_{USP} = 100 kN/mm/m², outer rail; — -: K_{USP} = 150 kN/mm/m², outer rail; - -: K_{USP} = 200 kN/mm/m², outer rail; —: no USP, inner rail; — —: K_{USP} = 100 kN/mm/m², inner rail; — -: K_{USP} = 150 kN/mm/m², inner rail; - -: K_{USP} = 200 kN/mm/m², inner rail).

The average changes in the overall stiffness w.r.t. the baseline scenario without USPs are listed in Table 3.

Table 3. Change in the overall stiffness wrt the baseline scenario without USPs.

	CEN56	NR60
Low USP stiffness	-23.0 %	-12.0 %
Medium USP stiffness	-17.0 %	-9.0 %
High USP stiffness	-12.0 %	-6.0 %
Average	-17.3 %	-9.0 %

From Figure 5(a) and Table 3, notice remarkable reductions in the overall track stiffness are found especially in case of the lowest USP stiffness, in line with expectations. This is a positive effect of the use of this supplementary layer as lower wheel/rail contact forces are expected. In addition, the USPs help to protect the ballast layer from damage as well as to increase the contact area between sleeper and ballast (see for example Abadi [21]).

In case of NR60 design (Figure 5(b) and Table 3), there are reasonable reductions in the overall track stiffness, especially in case of the lowest USP stiffness. This can be explained with the fact that the baseplate system already confers high resilience to the track form.

The effect of USPs on receptance curves of CEN56 and NR60 crossing designs is presented in Figure 6.

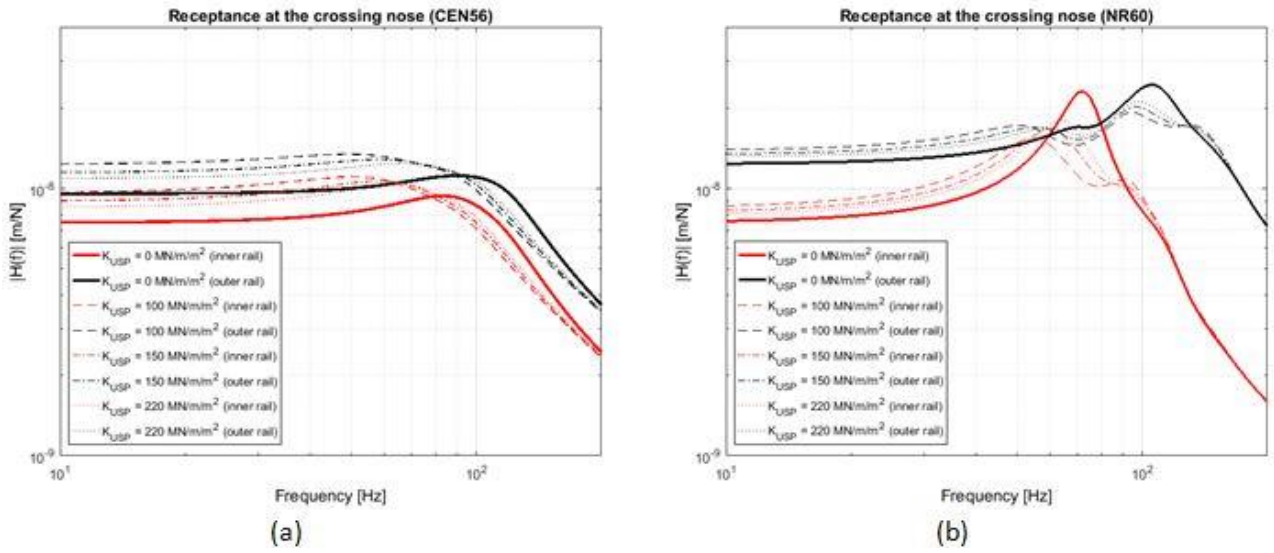

Figure 6. The effect of USPs on the frequency response curves in case of (a) CEN56 crossing and (b) NR60 crossing.

For CEN56 (Figure 6(a)), the use of added resilience changes the modal response at low frequencies (<200Hz), whereby the first resonance peak shift towards a lower frequency (from ca. 100Hz to ca. 60Hz) and becomes almost negligible (highly damped). For NR60 (Figure 6(b)) a similar trend is observed, with a shift towards a lower frequency and more damping for the first modal response, which remains more pronounced. Above 150 to 200Hz, the behaviour remains unaffected by USPs. In addition, the curves tend to be shifted towards higher receptance values (i.e. lower stiffness, as shown in Figure 5). Thus, from a practical point of view, the USPs contribute to the reduction of stiffness variation at the crossing panel but might also introduce potential resonance behaviour.

4. The dynamic system

4.1. Vehicle/track interaction model

A linearised three-dimensional vehicle/track interaction (VTI) model used to calculate the dynamic response of the system has been developed at University of Huddersfield and is shown in Figure 7.

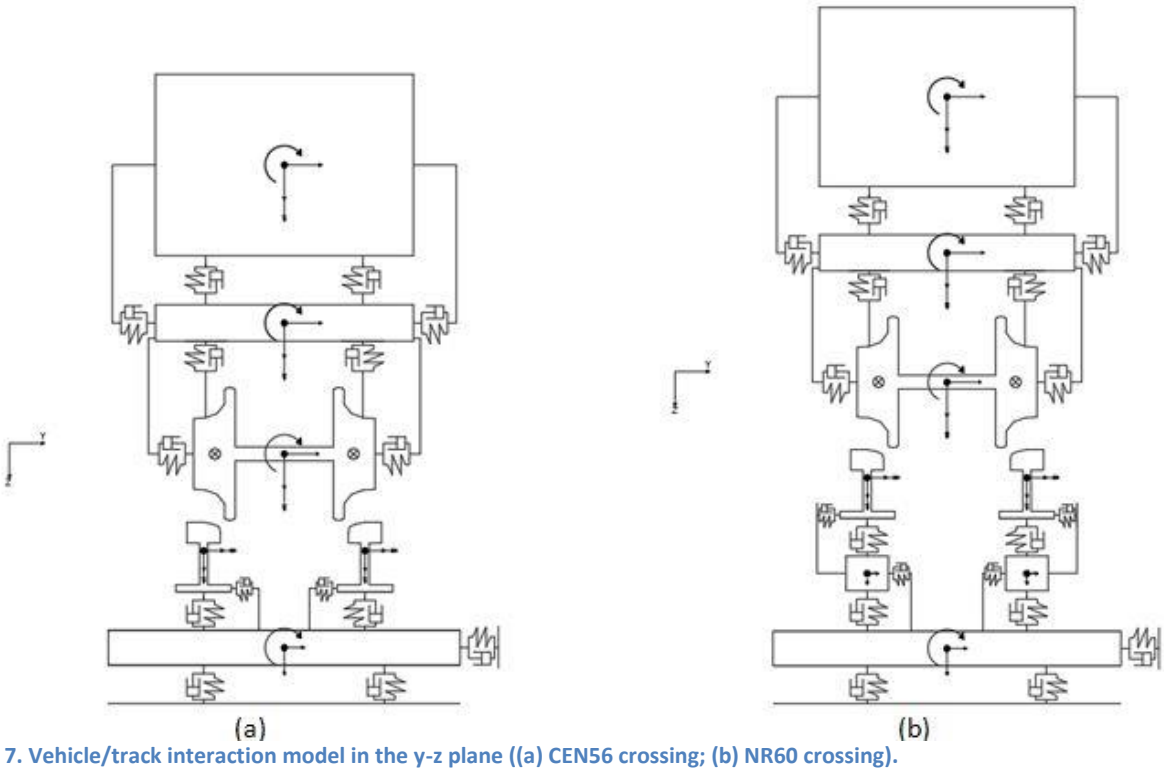

Figure 7. Vehicle/track interaction model in the y-z plane ((a) CEN56 crossing; (b) NR60 crossing).

The track is modelled as described in Section 3.

A rigid single axle, half bogie and quarter car-body are considered for this study. This model is able to capture the peak forces P1 and P2 (i.e. first and second impact at wheel transition as explained in Jenkins [22]), as well as creepages and creep forces using a limited number of DOFs. A comparison with the commercial software Vi-Rail has been carried out and a good agreement has been obtained (in the range + / - 8%) [23].

Each body is described by four DOFs: vertical and lateral displacements; roll and yaw rotations. Linear primary and secondary suspensions connect the wheelset with the bogie frame and the bogie frame with the car-body frame, respectively, in the longitudinal, lateral and vertical direction. The main freight vehicle parameters are reported in Table 4.

Table 4. Main vehicle input data [24].

Parameter	Value	Units
Wheel profile	UK P10 profile	
Wheelset mass	1500	kg
Wheelset yaw inertia	810	kg·m^2
Longitudinal primary suspension stiffness	1.8	KN/mm
Lateral primary suspension stiffness	1.8	KN/mm
Vertical primary suspension stiffness	5	KN/mm
Longitudinal secondary suspension stiffness	6.5	KN/mm
Lateral secondary suspension stiffness	6.5	KN/mm
Vertical secondary suspension stiffness	6	KN/mm
Equivalent static load per axle	22.5	t

The wheel-rail interface is modelled using contact elements taking into account the normal and tangential forces. The normal forces are modelled using the Hertzian theory [25] and the tangential forces using the Shen, Hedrick and Elkins theory [26].

Since the crossing panel is characterised by abrupt changes in rail profile geometry within a few meters, an online calculation is adopted, which consists on determining the wheel/rail contact data (i.e. the contact point, penetration between wheel and rail, contact angle and rolling radius) interpolating longitudinally the profiles at each integration time step. In this way it is possible to avoid the interpolation

between contact tables, which can easily cause remarkable errors when consecutive profiles with different width are considered.

It is necessary to highlight that in this study a two-dimensional search of the contact point is considered, neglecting the influence of wheelset yaw angle, which is acceptable since the optimisation study is carried out for through traffic only.

The contact position is thus found by searching the minimum vertical wheel-rail distance. In the range of the possible contact point, both profiles are re-interpolated with a cubic spline function in order to achieve a better precision.

An example of outputs in terms of contact forces and ballast force at the three points of control varying the speed is presented in Figure 8. The stars refer to the sleepers within the yellow and blue boxes in Figure 2(c) and the filled stars to the point of control.

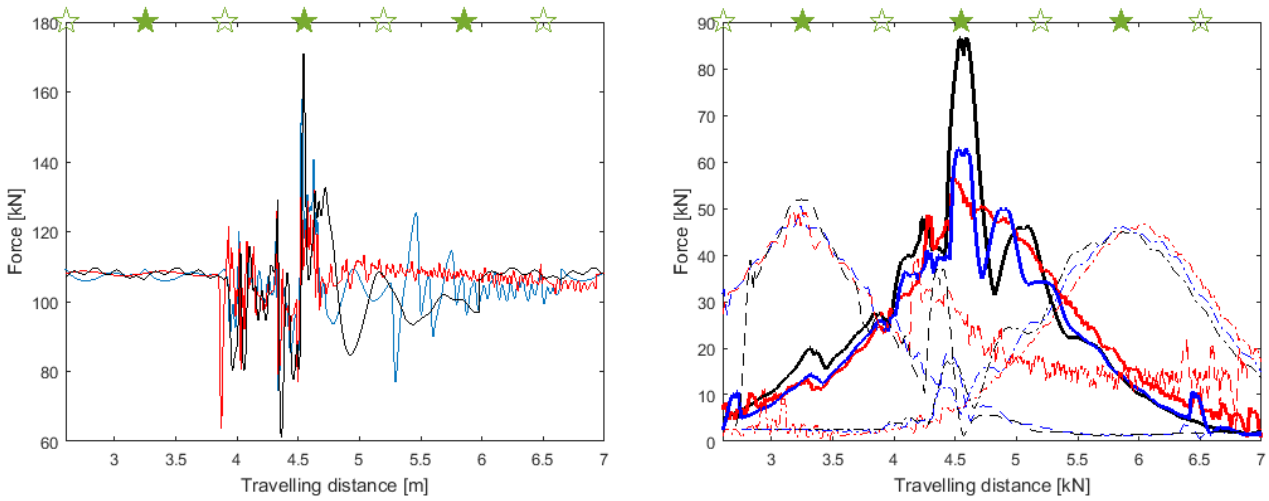

(a) (b)

Figure 8. Example of (a) contact forces along the crossing panel and (b) ballast forces at the three points of control at varying travelling speed (red lines: 40 km/h; blue lines: 80 km/h; black lines: 120 km/h).

It has been planned to validate the dynamic model established here against the field measurements taken at a UK site. The results will be presented in a following-up paper.

4.2. Optimisation routine

The outputs of the vehicle/track interaction model described in Section 4.1 are the inputs for the calculation of the long-term behaviour of the system. This is assessed through macro indices which can give an indication of severity, velocity and location of the degradation. Three main degradation modes associated with the most common causes of failures are considered: settlement of the ballast layer, wear and Rolling Contact Fatigue (RCF) of the rails and fatigue of the track components. The macro-indices examined are:

- *Settlement*: according to the literature (for example, [27-29]), the main drivers of the ballast settlement are sleeper accelerations and ballast pressure;
- *Wear/RCF*: In this study, excessive RCF and excessive wear are considered. In particular, RCF is considered excessive when the Tγ values (i.e. the sum of the product of creepages and corresponding creep forces [30]) are in the range between 30 N and 142 N and the wear is considered excessive when the Tγ values are greater than 207 N. These values are validated against normal grades of rail steel (i.e. R260) for plain line and on UK routes [31]. Change of material type and application to S&C might in practice necessitate a modified damaged function as the R260 steel grade is not commonly used in crossings due to the high wear and

plastic deformation rate. This has been done applying the methodology described in Burstow [32] considering cast manganese[4];

- *Fatigue in the components*: rail-pad forces and stresses on the rail foot are considered, as they are an indicator of potential rail-pad and fastening failures and possible transversal cracks on the crossing bottom in combination with corrosion and defects, respectively. In particular, the rail bending stresses have been calculated neglecting the shear section effects as $M \cdot z/I_{yy}$, where M is the bending moment, z the vertical position of the rail foot from the centroid and I the section second moment of area around the y axis.

Each of these macro-indices has been calculated as the relative difference between the 95th percentile of the case examined at the three points of control (shown in Figure 2(c) as stars) and the reference case, which is denoted with an asterisk in Equation 1.

The reference case for dynamic rail-pad stiffness is 200 KN/mm along the entire crossing panel for the CEN56 design and 50 KN/mm for the NR60 design, as well as in the plain line.

The objective function can be expressed as follows:

$$F(x) = \alpha \cdot \sum_{i=1}^{n_w} w_i \cdot \left(\frac{SA}{SA^*} - 1\right) + \beta \cdot \sum_{i=1}^{n_w} w_i \cdot \left(\frac{BP}{BP^*} - 1\right) + \gamma \cdot \sum_{i=1}^{n_w} w_i \cdot \left(\frac{Tgamma_{RCF}}{Tgamma_{RCF}{}^*} - 1\right) + \delta \cdot \sum_{i=1}^{n_w} w_i \cdot \left(\frac{Tgamma_{wear}}{Tgamma_{wear}{}^*} - 1\right) + \varepsilon \cdot \sum_{i=1}^{n_w} w_i \cdot \left(\frac{Stress_{foot}}{Stress_{foot}{}^*} - 1\right) + \theta \cdot \sum_{i=1}^{n_w} w_i \cdot \left(\frac{Force_{pad}}{Force_{pad}{}^*} - 1\right) \quad (1)$$

Where:

α, β, γ, δ, ε, θ = weight per each degradation mode considered;

n_w = number of wheel profiles considered (in this study equal to 3: new, moderately worn and worn P10);

w_i = weight of the i-th wheel profile (0.3 for the new wheel, 0.5 for the medium worn wheel, 0.2 for the heavily worn wheel);

SA = maximum sleeper acceleration at the three points of control (marked with a star in Figure 2(c)) and maximum sleeper acceleration at the three points of control in the nominal situation [m/s^2];

BP = maximum ballast pressure at the three points of control (marked with a star in Figure 2(c)) and maximum ballast pressure at the three points of control in the nominal situation [MPa];

$Tgamma_{RCF}$ = damage function value due to excessive RCF at the three points of control (marked with a star in Figure 2(c)) and damage function due to excessive RCF at the three points of control in the nominal situation;

$Tgamma_{wear}$ = damage function value due to excessive wear at the three points of control (marked with a star in Figure 2(c)) and damage function due to excessive wear at the three points of control in the nominal situation;

$Stress_{foot}$ = stress on the rail foot at the three points of control (marked with a star in Figure 2(c)) and stress on the rail foot at the three points of control in the nominal situation [MPa];

$Force_{pad}$ = maximum rail-pad forces at the three points of control (marked with a star in Figure 2(c)) and maximum rail-pad forces at the three points of control in the nominal situation [kN].

The optimum solution that minimises the total damage calculated due the passage of a wheelset over the crossing panel is found using a genetic algorithm by varying the rail-pad stiffness in case of direct fixing and the baseplate stiffness in case of indirect fixing.

Applying the genetic algorithm with an independent variable for each sleeper would lead to the most optimised solution. However, this can lead to a very high computational effort and therefore, in case of short crossings (i.e. crossing angle up to 1in9), it is advisable to use one optimisation variable, in case of medium crossings (i.e. crossing angle up to 1in15) two variables and in case of long crossings three or more

[4] The values considered are as for steel grade 350HT [31].

variables [19]. Since both the turnouts used in the simulations are medium turnouts (i.e. 1in13 and 1in11 crossing angle respectively (Table 2)), it has been decided to use two optimisation variables [19]. The first one X1 refers to the stiffness under the crossing nose area (blue box in Figure 2(c)) and the second X2 at the edge of the casting (yellow boxes in Figure 2(c)).

For the direct fixing, the range of dynamic stiffness considered is based on typical values for very soft, soft and medium railway pads (Table 1) from 30 to 300 KN/mm with a step of 10 KN/mm. For the indirect fixing, the range of dynamic stiffness considered is based on typical values for commercial baseplate-pads (Table 1) from 20 to 150 KN/mm with the same step of 10 KN/mm.

Regarding the constraints, it is necessary to guarantee that the change in the overall track stiffness is as smooth as possible in order to minimise the impact forces. Therefore, the variation in track stiffness between each sleeper pair should not exceed 30 %, while the rms-value of the stiffness distribution along the entire crossing panel should not exceed 20 %, thus ensuring homogeneity of stiffness along the crossing panel.

Note that in the following sections describing the sensitivity analysis (Section 4.3), the main results (Section 5.2) and the parametric study (Section 6) the facing direction of the through route (Figure 2) is considered, unless otherwise stated.

4.3. Initial sensitivity analysis of the objective function to the input parameters

In this Section, a sensitivity analysis has been performed in order to analyse the trend of each key indicator included in the objective function as well as their combination. It is worth underlying that the following discussions do not take in consideration the constraints.

On the direct fixing

Figure 9 shows the variation of the objective function for varying rail-pad stiffness between 30 and 300 kN/mm considering each damage mechanism at the time. The cases analysed refer to one travelling speed (80 km/h) representing average freight traffic in a medium turnout and average representative support stiffness (100 KN/mm). The black dot represents the nominal case (see the asterisk value in Eq. 1).

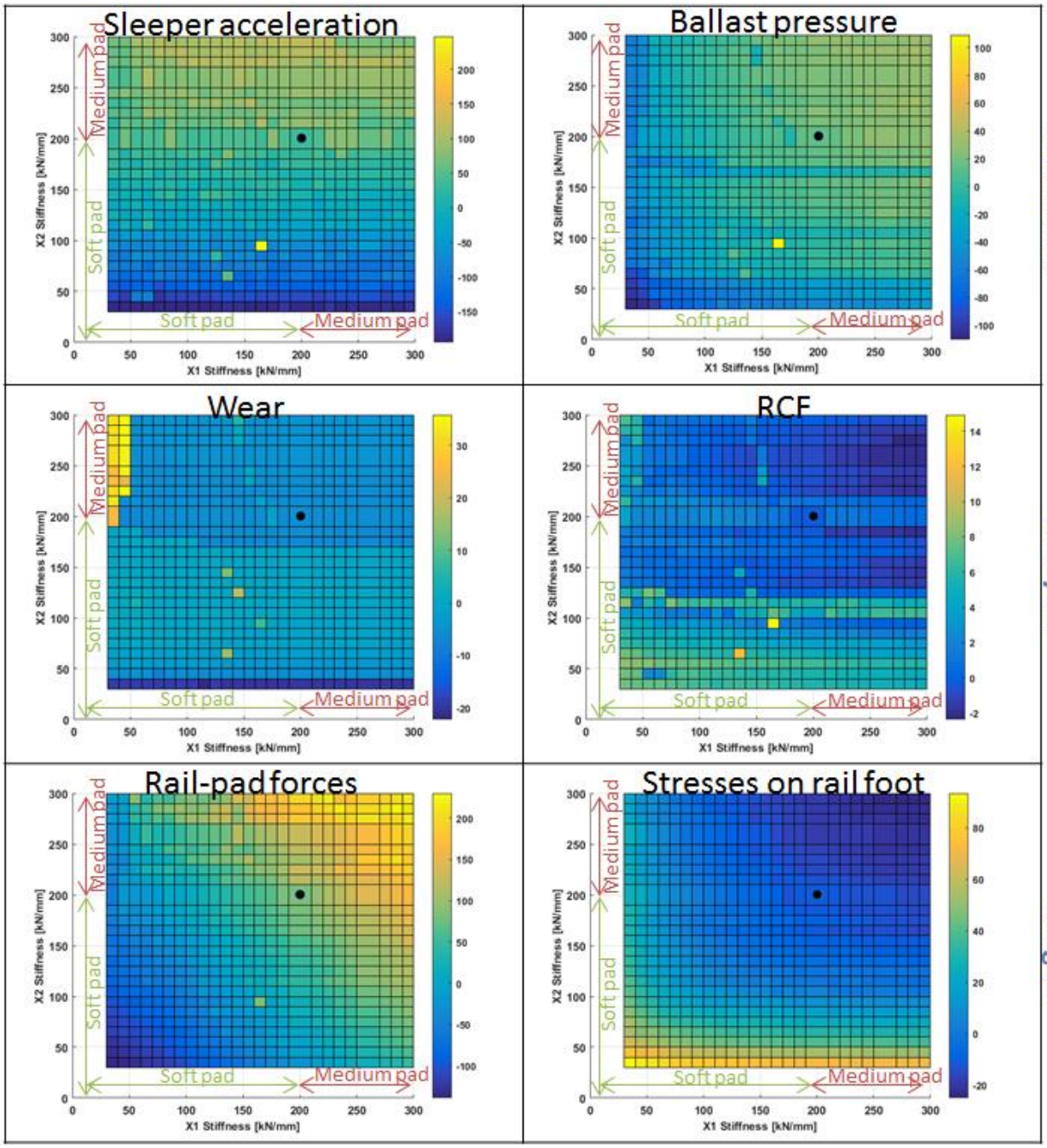

Figure 9. Percentage variation of the objective function relative to the value obtained for the combination of stiffness marked by the dot. Each damage mechanism is considered at a time [Speed = 80 km/h; Equivalent support stiffness = 100 kN/mm].

From a first analysis, it is possible to notice how all the key indicators analysed have different trends, sometimes in antithesis. Furthermore, the level of change of the key indicators varies significantly with the parameter considered, ranging between -140 % and +250 %. Therefore, a normalisation is necessary when all the terms considered are summed.

Looking in more detail to Figure 9, the following considerations can be drawn:

- Generally speaking, there are some very large deviations in the plot. This may be explained resonance behaviour using these pad stiffness values.
- Settlement
    - Sleeper acceleration: Using very soft pads for both variables leads to a decrease of ca. 150 % and using very stiff pads for both variables leads to an increase of about 60 %. The worst combination of pad stiffness is using soft/medium pads under the crossing nose area and

medium/stiff pads in the transition, leading to an increment of the sleeper acceleration of ca. 180 % w.r.t. the nominal case.
    - Ballast pressure: It is possible to identify a general decrease of ballast pressure with decreasing pad stiffness, as expected. The best combination is using the softest pads available all along the crossing panel, gaining a considerable 105 % improvement w.r.t. the nominal case.
- Wear/RCF
    - Wear: This quantity has a low susceptibility to the rail pad stiffness. Using soft pads in the crossing nose area and medium/stiff pads in the transition zone decreases the wear damage by about 20 %. The worst case scenario occurs with a combination of very soft pads under the crossing nose area and medium/stiff pads in the transition.
    - RCF: The RCF plot shows that this degradation mechanism decreases with increasing pad stiffness. The best combination is using the stiffest pads available all along the crossing panel, gaining a very modest 2 % improvement w.r.t. the nominal case.
- Fatigue in the components:
    - Rail-pad forces: Apart from some isolated cases, there is a general decrease of forces in the rail-pads with decreasing pad stiffness, as expected. The best combination is using the softest pads available, gaining a 130 % improvement w.r.t. the nominal case.
    - Stresses on the rail foot: On the contrary of the rail-pad forces, there is a general decrease of stresses with increasing pad stiffness, as the rail is less free to deform. The best combination is using the stiffest pads available, gaining a significant 20 % improvement w.r.t. the nominal case. However, it is only with very low pad stiffness that the absolute stress increase will become a problem.

On the indirect fixing

Figure 10 shows the variation of the objective function for varying baseplate stiffness between 20 and 150 kN/mm considering each damage mechanism at a time. The same travelling speed (80 km/h) and medium support stiffness (100 KN/mm) is used. The black dot represents the nominal case (see the asterisk value in Eq. 1).

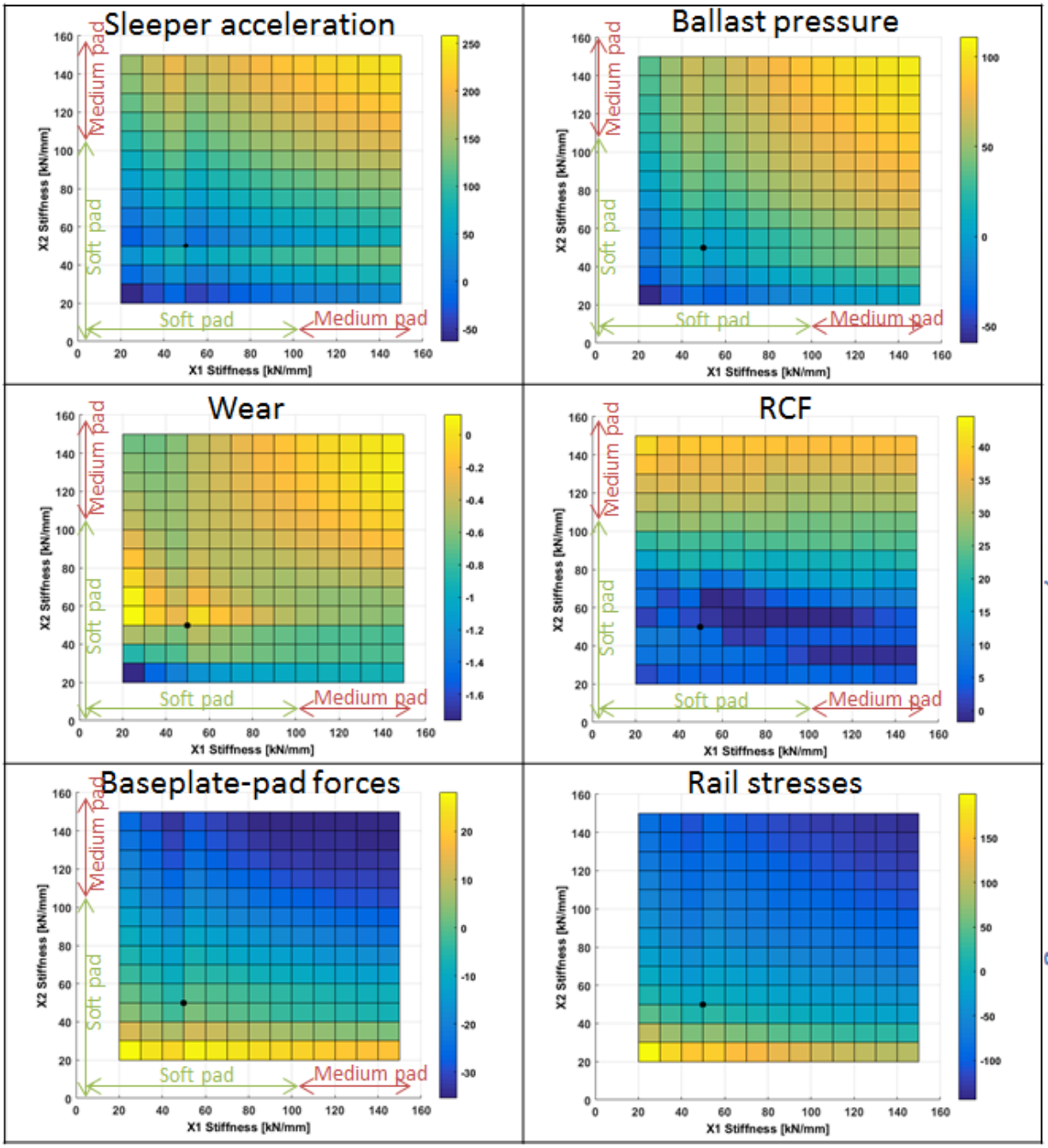

Figure 10. Percentage variation of the objective function relative to the value obtained for the combination of stiffness marked by the dot. Each damage mechanism is considered at a time [Speed = 80 km/h; Equivalent support stiffness = 100 kN/mm].

As in the case of direct fixing (Figure 9), Figure 10 shows that all the key indicators analysed have different trends with changes between -130 % and +260 %.

Looking in more detail, the following considerations can be drawn:

- Settlement
  - Sleeper acceleration: As for the direct fixing, the maximum decrease in sleeper acceleration happens when very soft baseplate-pads are used, while the maximum increase when stiff pads are used along the entire crossing panel. The variation occurring in this case is between -52 % and +260 %.
  - Ballast pressure: It is possible to identify a general decrease of ballast pressure with decreasing baseplate-pad stiffness, as previously shown. The best combination is using the softest pads available all along the crossing panel, gaining a considerable 53 % improvement w.r.t. the nominal case.

- Wear/RCF
  - Wear: A negligible decrease in wear (1.7 %) can be achieved using very soft baseplate-pads along the crossing panel. This can be explained with the fact that the wear is mainly dominated by the stiffness between the rail and the baseplate.
  - RCF: The RCF plot shows that the best solution is the nominal case, while using stiff pads leads to an increase of RCF of ca. 43 %.
- Fatigue in the components:
  - Baseplate-pad forces: Apart from some isolated cases, there is a general decrease of forces in the baseplate-pads with increasing pad stiffness. This trend is opposite to the case of direct fixing as in case of indirect fixing there are two stiffness values in series (i.e. connection between rail and baseplate, which is very stiff, and between baseplate and sleeper). The best combination is using the stiffest pads available, gaining a 130 % improvement w.r.t. the nominal case.
  - Stresses on the rail foot: As in case of the baseplate-pad forces, there is a general decrease of stresses with increasing pad stiffness, as the rail is less free to deform. The best combination is using the stiffest pads available, gaining a significant 35 % improvement w.r.t. the nominal case.

In Table 5 a summary of the findings for the separated indicators is presented.

Table 5. Summary of findings in terms of best solution and maximum improvement achievable per each indicator considered.

Degradation mode	Indicator	Best solution direct fixing	Improvement (w.r.t. nominal case)	Best solution Indirect fixing	Improvement (w.r.t. nominal case)
Settlement	Sleeper acceleration	Soft (entire panel)	-150 %	Soft (entire panel)	-52 %
	Ballast pressure	Soft (entire panel)	-105 %	Soft (entire panel)	-53 %
Wear/RCF	Wear	Soft (crossing nose area)+medium/stiff (transition)	-20 %	Soft (entire panel)	-1.7 %
	RCF	Medium/stiff (entire panel)	-2 %	Nominal case	0 %
Fatigue	Rail-pad forces	Soft (entire panel)	-130 %	Stiff (entire panel)	-130 %
	Stresses on rail foot	Medium/stiff (entire panel)	-20 %	Stiff (entire panel)	-35 %

5. Resilience optimisation results

5.1. Factoring the failure frequency and risk

In the previous Section, it has been demonstrated theoretically that the objective function is very complex as the damage indices considered have different trends, sometimes in antithesis, and the range of variation differs considerably.

Looking at the failure modes, Figure 11 shows the frequency distribution of potential failure modes at the crossing panel based on UK data for 2009 ([33]).

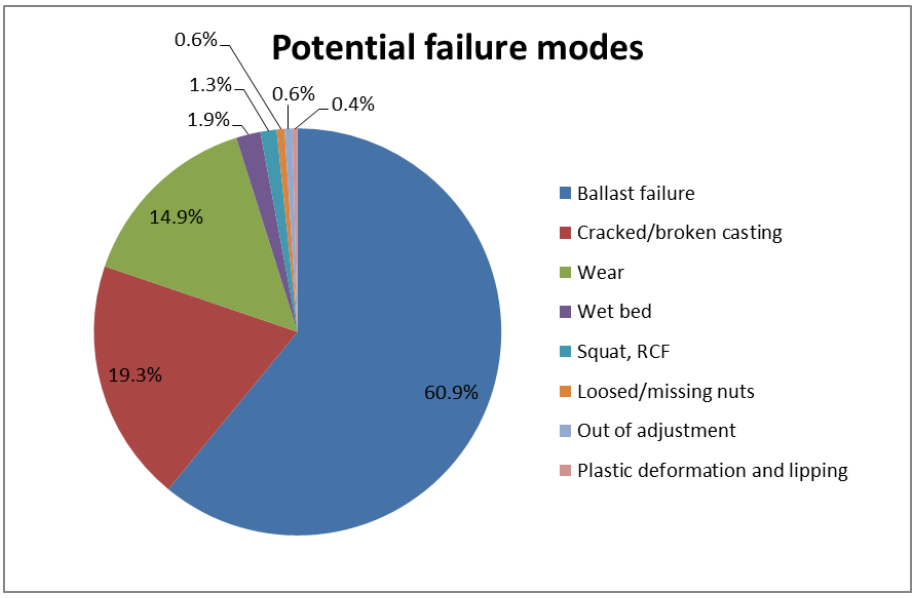

Figure 11. Frequency distribution of potential failure modes at the crossing panel [33].

The very high occurrence of voiding (i.e. ballast failure) at the crossing panel can be explained with the fact that the tamping in that region is not as straightforward as in plain line due to layout restriction. Some of the tines may hit an obstruction such as the switch blade or curved closure rail of the turnout portion. Sometimes, special tamping units (i.e. slit tamping units) are used, although additional time is required. Thus, it happens that they are not regularly tamped due to time restrictions during possession period, in addition to significant impact load occurring in this location. Voiding leads to a vicious cycle, as poor support conditions may cause increased loads and additional degradation in the ballast layer.

Regarding the cracked/broken casting failure mode, the occurrence is lower than the previous category, but the sensitivity (i.e. the severity of the effect of the failure mode) is extremely high, as there is a loss of the primary functionality and the operations may become unsafe.

A Failure Modes and Effects Analysis (FMEA) has been carried out in order to calculate the weighting per each damage mechanism considered in the objective function. The Risk Priority Number (RPN) quantifies the overall risk of a particular failure mode occurring in the system and is estimated as the product of the probability number P (i.e. how probable the failure considered is), the sensitivity number S (i.e. how sensible the failure considered is if occurred) and the detection number D (i.e. how easy to be detected the failure considered is). The values have been estimated as in Hassakiadeh [33] and the results are shown in Table 6.

Table 6. Calculation of the weights of the degradation modes considered in the objective function.

Degradation mode	Occurrence [%]	P [-]	S [-]	D [-]	RPN [-]
Ballast failure	60.9 %	5	3	2	30
Cracked/broken casting	19.3 %	4	5	3	60
Wear	14.9 %	3	4	2	24
Wet bed	1.9 %	2	2	1	4
Squat, RCF	1.3 %	2	2	2	8
Loosed/missing nuts	0.6 %	2	2	2	8
Out of adjustment	0.6 %	2	4	2	16
Plastic deformation and lipping	0.4 %	2	4	2	16

For the sake of simplicity, only the two degradation mechanisms with the highest RPN, which are the ballast failure and the cracked/broken casting, are considered.

These considerations have led to the simplified objective function as follows:

$$F(x) = 0.3 \cdot \sum_{i=1}^{n_w} w_i \cdot \left(\frac{BP}{BP^*} - 1\right) + 0.7 \cdot \sum_{i=1}^{n_w} w_i \cdot \left(\frac{Stress_{foot}}{Stress_{foot}^*} - 1\right) \quad (2)$$

where the weights of the degradation modes considered are calculated as the percentage of the RPN considered.

5.2. Comparing the direct and indirect fixing

Considering medium travelling speed (80 km/h) and medium support stiffness (100 KN/mm) as in Section 4.3, an example of results in terms of objective function value, optimisation parameters and track stiffness relative to the line track stiffness for direct fixing and indirect fixing is shown in Figure 12(a,b) and Figure 12(c,d), respectively. The red dot refers to the nominal case, the green dot to the optimised pad stiffness and the black dots to the value considered at the generic iteration.

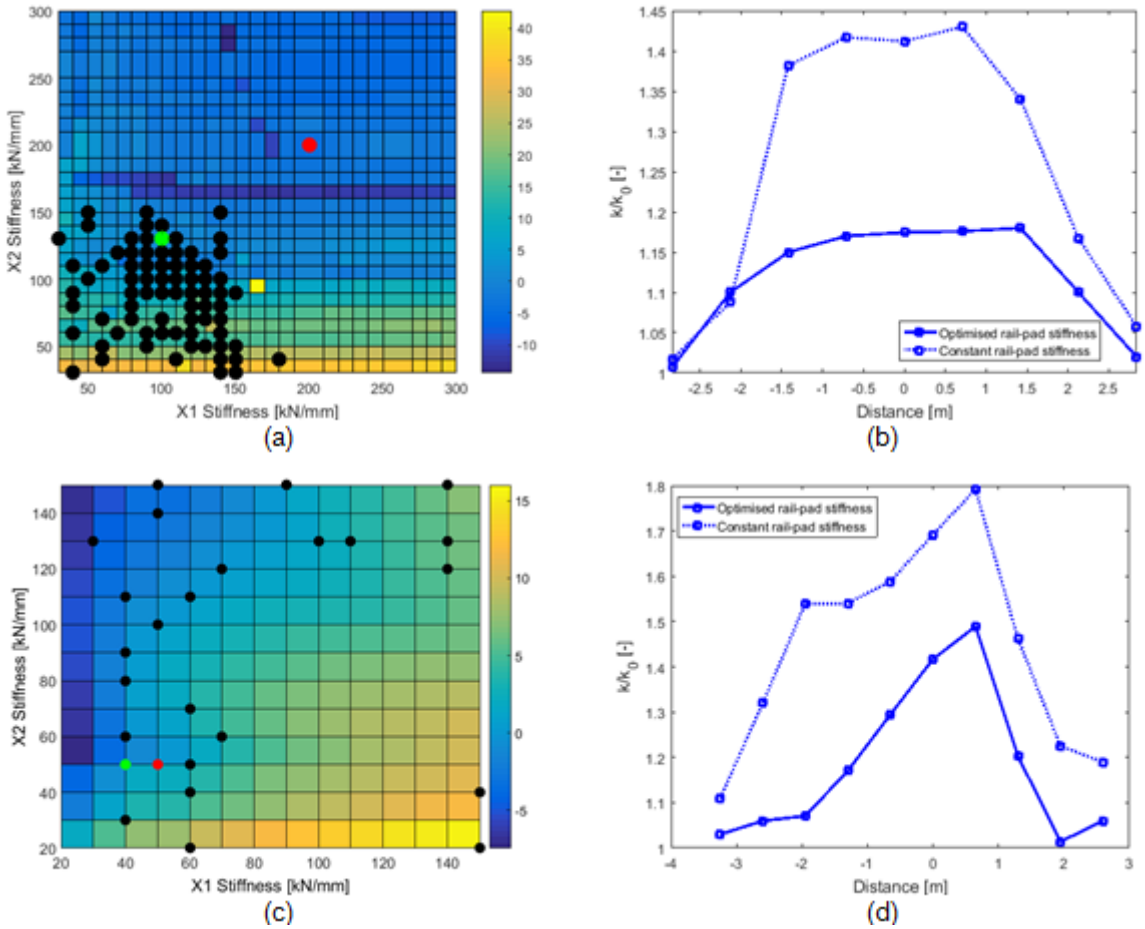

Figure 12. Example of results: objective function value and optimisation parameters for (a) direct fixing and (c) indirect fixing; track stiffness relative to the line track stiffness for (b) direct fixing and (d) indirect fixing [Speed = 80 km/h; Equivalent support stiffness = 100 kN/mm].

In case of direct fixing, the best solution appears to be soft/medium rail-pad stiffness along the entire crossing panel, namely 100 KN/mm under the crossing nose area and 130 KN/mm in the transition as dynamic values. If the dynamic/static ratio is assumed to be 1.4 (Table 1), these values correspond to 71 KN/mm and 93 KN/mm, respectively, as static pad stiffness. In this way, it is possible to have a gradual variation of track stiffness from the line to the crossing panel, as shown in Figure 12(b), as well as reducing the damage mechanisms of ca. 9 % w.r.t. the nominal case (Figure 12(a)). In particular, there is a reduction of ca. 36 % in ballast forces and an increase of ca. 2 % in bending stresses.

In case of indirect fixing, the optimum case results to be 40 KN/mm under the crossing nose area and 50 KN/mm in the transition as dynamic values of the baseplate-pads. These values do not differ a lot from the nominal case, as much softer pads would lead to additional bending stresses and, therefore, to an increase in the bending stresses and damage mechanisms. Nevertheless, using a slightly softer pad, it is possible to achieve already a beneficial decrease in damage mechanisms (namely ca. -2 %, which

corresponds to a reduction of ca. 9.5 % in ballast forces and an increase of ca. 1 % in bending stresses) as well as a better homogenisation of the track support stiffness (Figure 12(c,d)).

6. Parametric study

In Ishak [34], some factors influencing the rail degradation process have been identified, including the axle load, the traffic type, the traffic density, the speed, the ballast cleaning and rail profile.

The influence of the vehicle parameters (i.e. direction of travel and speed) is analysed in Section 6.1 and the influence of track parameter (i.e. track support stiffness) in Section 6.2.

6.1. Vehicle parameters

Direction of travel

The direction of travelling may affect the optimum pad stiffness values. The results of the sensitivity analysis for trailing direction in case of direct fixing are presented in Figure 13(a) and in case of indirect fixing in Figure 13(b) for a speed equal to 80 km/h and equivalent support stiffness equal to 100 KN/mm. The starting point is marked in red, the optimum value for the case of facing direction in green, the optimum value for the case of trailing direction in yellow and the black dots to the value considered at the generic iteration.

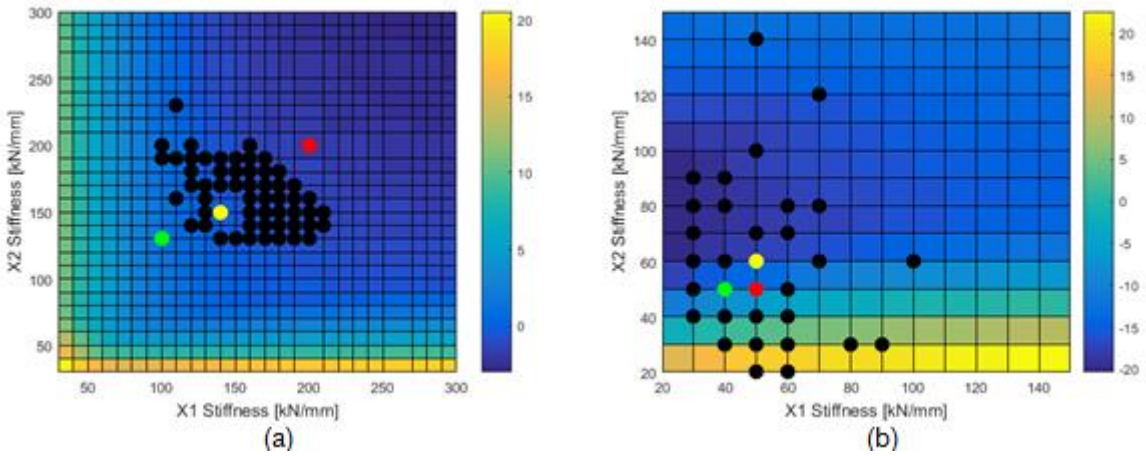

Figure 13. Results in terms of optimised pad stiffness values in the trailing direction ((a): direct fixing; (b); indirect fixing) [Speed = 80 km/h; Equivalent support stiffness = 100 kN/mm].

Comparing the results in the facing and trailing direction in case of direct fixing (Figure 12(a) and Figure 13(a)), it is possible to conclude that the trailing direction requires slightly stiffer pads. The optimum solution found is having the stiffness equal to 140 KN/mm along the entire crossing panel, which is in between the initial pad stiffness value and the one obtained for the facing direction. Moreover, the achieved gain of performance is not as important as for the facing direction. This can be explained with the fact that travelling in the trailing direction causes slightly higher impact forces and vibrations along the crossing and, thus, a slightly stiffer connection between rail and sleeper is required in order to limit the bending stresses. An overall optimised value would need to factor in both direction of travel depending on the traffic knowledge.

Similarly, in case of indirect fixing (Figure 12(c) and Figure 13(b)) the trailing direction requires slightly stiffer pads than the facing direction (i.e. 50 KN/mm along the crossing nose area and 60 KN/mm in the transition).

Travelling speed

Three speed cases, which are 40, 80 and 120 km/h, are discussed in this Section. The equivalent support stiffness is assumed to be 100 KN/mm.

Figure 14(a) shows the influence of support stiffness on the optimised pad stiffness values for typical track bed in case of direct fixing and Figure 14(b) in case of indirect fixing.

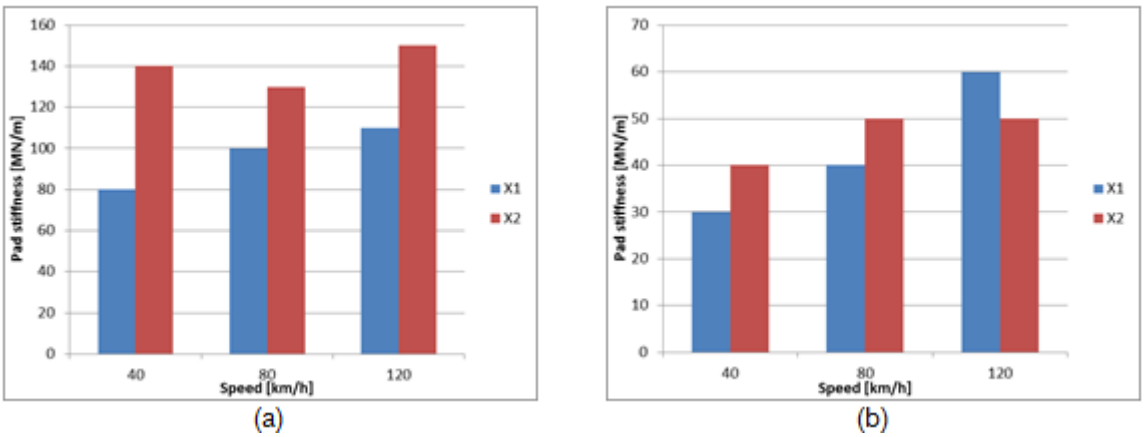

Figure 14. The influence of travelling speed on the optimised pad stiffness values for typical track bed ((a): direct fixing; (b) indirect fixing) [Equivalent support stiffness = 100 kN/mm].

For both types of fixing systems, an increase in the line speed requires an increase of rail-pad stiffness under the crossing nose area. This can be explained with the fact that trains travelling at higher speeds produce higher vibrations, so that a stiffer support is then required to prevent the propagation of these to the superstructure and, therefore, further damage.

On the other hand, the resulting optimum stiffness in the transition remains practically constant.

6.2. Track parameters

Three cases of track bed (i.e. soft, typical and stiff track bed) are analysed and the equivalent stiffness values are 40, 80, and 200 KN/mm, as suggested in the EUROBALT project [20].

Figure 15(a) shows the influence of support stiffness on the optimised pad stiffness values at 80 km/h in case of direct fixing and Figure 15(b) in case of indirect fixing.

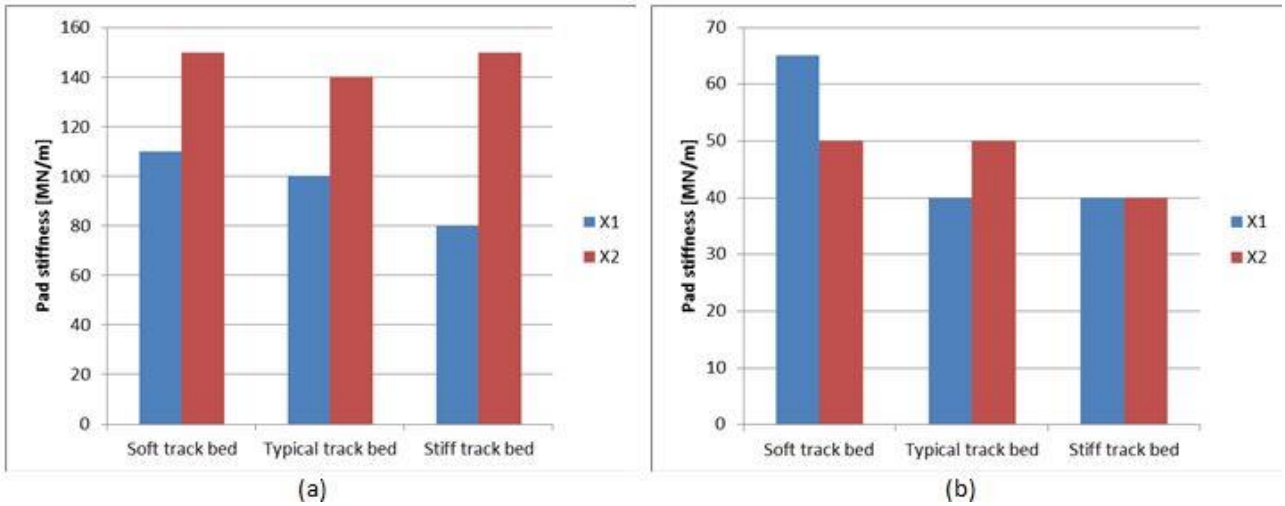

Figure 15. The influence of support stiffness on the optimised pad stiffness values ((a): direct fixing; (b); indirect fixing) [Speed = 80 km/h].

As expected, softer track support requires stiffer connections at the fixing level, especially when bending stresses are considered. This takes place especially in case of indirect fixing, since it already confers high resilience to the track form.

7. Conclusions and further work

In the building of railway switches and crossings, there are two main ways of linking the rail to the sleeper: direct fastening and indirect fastening. This paper presents, in the context of a crossing panel, a comparison between these two fastening types in terms of the equivalent system stiffness variation with distance, track frequency response and eventual dynamic optimisation of track support acting on rail pad properties.

The distribution of equivalent system stiffness shows that there is a remarkable increase at the crossing panel with respect to plain line, due to significantly higher bending stiffness of the casting as well as the presence of long bearers and additional rails. In the case of indirect fixing, the increased bending stiffness of the casting is partially counterbalanced by the higher resilience given by the baseplate system. The effect of USPs has been analysed and the highest reductions of track stiffness gradient occur when applied to a system with direct fixing.

A methodology to optimise pad stiffness in the crossing panel, minimising the most common degradation modes and guaranteeing a smooth distribution of total track stiffness has been established. A three-dimensional vehicle/track interaction model has been used in order to evaluate the dynamic behaviour of a half vehicle negotiating the crossing panel. The proposed model includes an accurate description of the track structure using beam on discrete support, which is often approximated with co-running track models in commercial vehicle dynamics simulation programs.

The contribution of each indicator considered in the objective function is analysed in detail for different combination of pad stiffness, both in case of direct and indirect fixing. In the first situation and using the softest pads, it is possible to minimise the ballast pressure (linked with track settlement), the excessive contact patch energy (linked with wear and RCF) and the rail-pad forces (linked with component fatigue). With the stiff pads the stresses on the rail head and foot (linked with component fatigue) are minimised. The maximum achievable reductions vary from 2 % to 150 %. Similar results are obtained for fatigue indices in the case of the indirect fixing, but the benefits are less significant for ballast and rail head damage indices.

Based on the frequency distribution of representative failure modes and their severity, an optimisation analysis was performed restricting the scope to ballast degradation and the fatigue of the casting. It has demonstrated how it is possible to drastically improve the crossing performance finding the

optimum value of pad stiffness, in some cases reaching 30 % reduction in equivalent system stiffness along the crossing panel w.r.t. the reference case and 13 % reduction in the objective function value. In case of indirect fixing, the optimum values do not differ a lot from the nominal case, because much softer pads would lead to unreasonable additional bending stresses and potential for fatigue failures.

The influence of speed, travelling direction and ballast support stiffness has been considered on the overall results. As a general rule, an increase in the line speed requires an increased pad stiffness, while an hardly compacted ballast support stiffness requires a decrease in pad stiffness, especially in case of direct fixing. There is therefore a natural trade-off to be considered and any optimisation would need to consider altogether the specific conditions in which the crossing will be utilised.

As further work, it may be beneficial to assess the influence of axle load. In the present study, the pad stiffness has been modelled as linear. It would be useful to develop a non-linear model also considering the frequency-dependent response of the system. It is also important to evaluate the effect of USPs as they have a strong influence on the overall system behaviour but may lead to excessive dynamic amplifications. Finally, the sleeper acceleration as well as the wear and RCF degradation modes should be included in the objective function.

Acknowledgement

This work was supported by the European Commission within the FP7 Capacity4Rail project [Grant n. 605650] and EPSRC Track to the Future project [Grant n. EP/M025276/1].

References

1. Lichtenberger, B., *Track compendium*. 2011, Hamburg: Eurail Press.
2. Kassa, E., C. Andersson, and J.C. Nielsen, *Simulation of dynamic interaction between train and railway turnout.* Vehicle System Dynamics, 2006. **44**(3): p. 247-258.
3. Nicklisch, D., et al., *Geometry and stiffness optimization for switches and crossings, and simulation of material degradation.* Proceedings of the Institution of Mechanical Engineers, Part F: Journal of Rail and Rapid Transit, 2010. **224**(4): p. 279-292.
4. Ekberg, A. and B. Paulsson, *INNOTRACK: concluding technical report*. 2010: International Union of Railways (UIC).
5. Pålsson, B.A. and J.C.O. Nielsen, *Dynamic vehicle–track interaction in switches and crossings and the influence of rail pad stiffness–field measurements and validation of a simulation model.* Vehicle System Dynamics, 2015. **53**(6): p. 734-755.
6. Markine, V., M. Steenbergen, and I. Shevtsov, *Combatting RCF on switch points by tuning elastic track properties.* Wear, 2011. **271**(1): p. 158-167.
7. Bruni, S., et al., *Effects of train impacts on urban turnouts: Modelling and validation through measurements.* Journal of Sound and Vibration, 2009. **324**(3–5): p. 666-689.
8. Bezin, Y., *SUSTRAIL D4.4: Optimised switches and crossing systems*. 2014.
9. Wan, C., V. Markine, and I. Shevtsov, *Optimisation of the elastic track properties of turnout crossings.* Proceedings of the Institution of Mechanical Engineers, Part F: Journal of Rail and Rapid Transit, 2016. **230**(2): p. 360-373.
10. Asmussen, B., *RIVAS D.3.6: Description of the vibration generation mechanism of turnouts and the development of cost effective mitigation solutions*. 2013.
11. Network Rail, *RT/CE/S/052 Rail and baseplate pads*. 2002: London.
12. European Committee for Standardization, *EN 13146 Railway applications - Track - Test methods for fastening systems - Part 9: Determination of stiffness*. 2009: Brussels.

13. European Committee for Standardization, *EN 14363 Railway applications - Testing and simulation for the acceptance of running characteristics of railway vehicles - Running Behaviour and stationary tests*. 2016: Brussels.

14. European Committee for Standardization, *EN 13481 Railway applications - Track - Performance requirements for fastening systems - Part 2: Fastening systems for concrete sleepers*. 2012: Brussels.

15. European Committee for Standardization, *EN 13481 Railway applications - Track - Performance requirements for fastening systems - Part 3: Fastening systems for wood sleepers*. 2012: Brussels.

16. European Committee for Standardization, *EN 13481 Railway applications - Track - Performance requirements for fastening systems - Part 4: Fastening systems for steel sleepers*. 2012: Brussels.

17. European Committee for Standardization, *EN 13481 Railway applications - Track - Performance requirements for fastening systems - Part 5: Fastening systems for slab track with rail on the surface or rail embedded in a channel*. 2012: Brussels.

18. Network Rail, *NR/L2/TRK/2049 Track design handbook*. 2010: London.

19. Grossoni, I., Y. Bezin, and S. Neves, *Optimization of support stiffness at a railway crossing panel*, in *The third Conference on Railway Technology: Research, Development and Maintenance*, J. Pombo, Editor. 2016, Civil-Comp Press: Cagliari (Italy).

20. Hunt, G.A., *EUROBALT: vertical dynamic model for track damage studies*. 1996, British Rail Research.

21. Abadi, T., et al., *Measuring the area and number of ballast particle contacts at sleeper/ballast and ballast/subgrade interfaces.* The International Journal of Railway Technology, 2015. **4**(2): p. 45-72.

22. Jenkins, H.H., et al., *The effect of track and vehicle parameters on wheel/rail vertical dynamic forces.* Railway Engineering Journal, 1974. **3**(1).

23. Grossoni, I., *Design methodology for innovative track systems - PhD First year report*. 2015.

24. Zhai, W., *Vehicle-track coupling dynamics.* Beijing, China: Science Publishing House, 2007: p. 12-132.

25. Hertz, H., *Über die Berührung fester elastischer Körper.* Journal Fur Die Reine Und Angewandte Mathematik 1882. **1882**(92): p. 16.

26. Shen, Z.Y., J.K. Hedrick, and J.A. Elkins, *A comparison of alternative creep force models for rail vehicle dynamic analysis.* Vehicle System Dynamics, 1983. **12**(1-3): p. 79-83.

27. Demharter, K., *Setzungsverhalten des Gleisrostes unter vertikaler Lasteinwirkung*. 1982: Prüfamt für Bau von Landverkehrswegen d. Techn. Univ. München.

28. Guerin, N., *Approche expérimentale et numérique du comportement du ballast des voies ferrées*. 1996, Ecole Nationale des Ponts et Chaussées.

29. Sato, Y., *Japanese Studies on Deterioration of Ballasted Track.* Vehicle System Dynamics, 1995. **24**(sup1): p. 197-208.

30. Burstow, M.C., *Whole Life Rail Model application and development of RSSB - Continued development of an RCF damage parameter*. 2004, Rail Safety and Standards Board.

31. Evans, J., T. Lee, and C. Hon, *Optimising the wheel/rail interface on a modern urban rail system.* Vehicle System Dynamics, 2008. **46**(S1): p. 119-127.

32. Burstow, M.C., *Proposed new WLRM damage function for alternative rail materials*. 2009, Network Rail.

33. Hassankiadeh, S.J., *Failure Analysis of Railway Switches and Crossings for the purpose of Preventive Maintenance*, in *Department of Transport Science*. 2011, Royal Institute of Technology (KTH): Stockholm.

34. Ishak, M.F., S. Dindar, and S. Kaewunruen. *Safety-based Maintenance for Geometry Restoration of Railway Turnout Systems in Various Operational Environments*. in *Proceedings of The 21st National Convention on Civil Engineering*. 2016.